



POLITECNICO
MILANO 1863

SCUOLA DI INGEGNERIA INDUSTRIALE
E DELL'INFORMAZIONE

EXECUTIVE SUMMARY OF THE THESIS

Thermodynamic Modelling and Component Sizing of Wastewater Source Heat Pump for District Line Including On - Off Design Analysis and CO₂ Reduction Assessment

LAUREA MAGISTRALE IN ENERGY ENGINEERING - INGEGNERIA ENERGETICA

Author: ANGELICA CORTINOVIS

Advisor: PROF. PAOLO CHIESA

Academic year: 2024-2025

1. Abstract

This thesis develops and applies a thermodynamic modelling framework for a wastewater source heat pump, using in hybrid configuration with an electric boiler to cover the residual heat demand, integrated into a district heating network. The heat pump cycle is modelled at on design conditions, including component sizing, and subsequently extended to off design operation. Then, the overall hybrid system is analysed through annual simulations performed using the off design model under time varying wastewater availability and heat demand profiles, in order to identify the heat supply configuration that maximises CO₂ emission savings. The proposed methodology therefore represents a robust tool to identify the urban contexts in which wastewater source heat pumps can be most effectively integrated.

2. Introduction

The decarbonisation of urban heating represents a key challenge of the energy transition, as district heating networks in many European cities are still largely supplied by fossil fuel based technologies [1]. In this context, wastewater source

heat pumps offer a promising solution, since urban sewer systems provide a stable and locally available low temperature heat source [2].

The integration of wastewater heat recovery into district heating networks can therefore contribute to reducing the carbon intensity of urban heat supply. However, large scale deployment, requires robust modelling tools capable of capturing both nominal and seasonal performance under time varying heat demand and wastewater availability. In the specific case of Milan, previous studies carried out by the local utility *MM S.p.A.* have investigated the decarbonisation of district heating supply through CHP based solutions [3] and assessed the feasibility of wastewater heat recovery [4].

The present work is a modelling based extension of this real urban context, building upon existing infrastructure and realistic boundary conditions for the city of Milan. It advances the analysis through the development of a detailed on design and off design modelling framework coupled with annual simulations, providing a quantitative and system level assessment of the potential contribution of wastewater source heat pumps to energy savings and CO₂ emission reduction under realistic operating conditions.

3. System Overview

The overall hybrid heat supply system considered in this work, shown in Figure 1, consists of a heat pump supplying the district heating network and an electric boiler covering the residual heat demand.

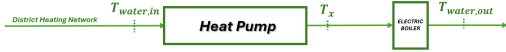


Figure 1: Hybrid configuration of the system.

The wastewater heat pump cycle configuration is shown in Figure 2. The cycle exploits wastewater as low temperature heat source and delivers thermal energy to the district heating network on the sink side. A double vapour compression layout with intermediate flash tank is adopted to improve compressor operating conditions, by splitting the overall compression into two stages, and cycle efficiency [5]. The working fluid selected for the heat pump is R1234ze, due to its favourable thermophysical properties and low environmental impact ($GWP = 4$) in the investigated operating temperature range [6].

The main components of the heat pump system include the evaporator and superheater on the source side, two centrifugal compressors with intermediate mixing, an intermediate flash tank, the desuperheater, condenser and subcooler on the sink side, and two expansion valves. An intermediate water loop, with its dedicated pump, is interposed between the wastewater stream and the heat pump in order to ensure hydraulic separation and operational flexibility.

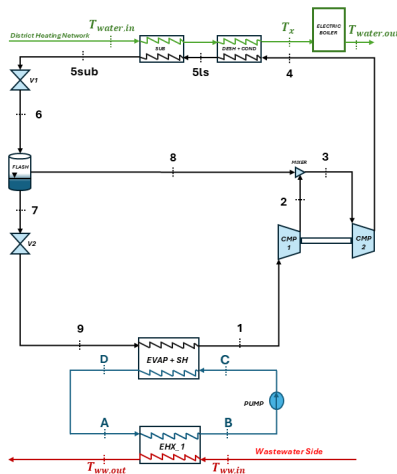


Figure 2: Layout of the system.

4. Modelling Framework: On-Off Design and Sizing

A modelling framework is developed to describe the thermodynamic behaviour of the wastewater source heat pump under both on design and off design conditions, implemented through dedicated numerical algorithms. The on design model is employed to determine the nominal operating point and to size the main components of the cycle, while the off design model is formulated to capture the system response to variable boundary conditions on the source and district heating network.

4.1. On Design Procedure

Algorithm 1 On design modelling workflow

- 1: Read inputs and initialize T_{cond}
- 2: **repeat**
- 3: Solve thermodynamic cycle
- 4: Update T_{cond} (thermal closure)
- 5: **until** convergence on T_{cond}
- 6: Final evaluation of cycle performance (COP, powers)
- 7: Compressor map matching
- 8: Heat exchanger sizing

Cycle and Compressors Modelling

The heat pump cycle is modelled under on design conditions to determine a consistent nominal operating point of the heat pump. The on design analysis is carried out under a set of general modelling assumptions, including steady state operation, adiabatic components and prescribed pressure losses, and starting from fixed boundary conditions representative of the wastewater source, the district heating network, and selected characteristic temperature differences ΔT imposed across the main heat exchangers of the system. The main boundary conditions adopted are summarised in Table 1.

Symbol	Value	Unit
$T_{\text{ww},\text{in}}$	14	$^{\circ}\text{C}$
$T_{\text{ww},\text{out}}$	10	$^{\circ}\text{C}$
\dot{m}_{ww}	100	L/s
$\Delta T_{\text{pp,EHX}_1}$	5	K
$\Delta T_{\text{ap,sub}}$	8	K
$\Delta T_{\text{ap,cond}}$	5	K
ΔT_{sh}	5	K

Table 1: Main boundary conditions adopted in the on-design analysis.

As a preliminary step of the on design modelling,

the thermal power available from the wastewater stream \dot{Q}_{ww} is evaluated and transferred to an intermediate water loop. The corresponding mass flow rate \dot{m}_{int} and temperature levels of the intermediate circuit (T_a , T_b , T_c , T_d) are determined through energy balances across the wastewater heat exchanger and the evaporator, consistently with the prescribed pinch-point temperature differences. The circulation pump power $\dot{W}_{\text{pump,mech}}$ required to overcome hydraulic losses in the intermediate loop is also accounted for. On this basis, the evaporating temperature of the refrigerant T_{evap} and the outlet temperature at the evaporator, T_1 , are defined. Starting from this two inputs, the thermodynamic state points of the heat pump cycle, represented in Figure 3, are reconstructed by applying the component level thermodynamic relations.

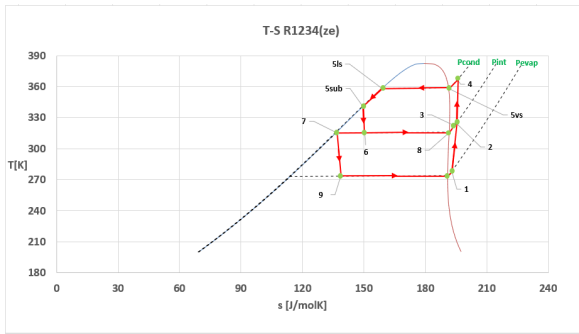


Figure 3: T-s diagram of the thermodynamic cycle.

For each point, thermodynamic properties as T, P, h, s, x are calculated using *REFPROP* functions. Since the reconstruction of the cycle state points requires also the condensing temperature as an input, the cycle calculation is embedded within an iterative procedure on T_{cond} . At each iteration n , the condensing temperature is updated according to the thermal closure condition at the condenser:

$$T_{\text{cond}} = T_x + \Delta T_{\text{ap,cond}}, \quad (1)$$

where T_x is the district heating water temperature at the desuperheater outlet; until the convergence criterion:

$$\left| T_{\text{cond}}^{(n+1)} - T_{\text{cond}}^{(n)} \right| < \varepsilon \quad (2)$$

is satisfied. Upon convergence, a final simulation run is performed to update the thermodynamic state points of the cycle and to evaluate

the thermal duties of the heat exchangers:

$$\dot{Q}_i = \dot{m}_i (h_{i,\text{out}} - h_{i,\text{in}}), \quad (3)$$

where

$$i = \{\text{evap, sh, desh, cond, sub}\}$$

and the mechanical power of the two compressor stages:

$$\dot{W}_{\text{cmp},j} = \dot{m}_j (h_{j,\text{out}} - h_{j,\text{in}}), \quad j = 1, 2. \quad (4)$$

The corresponding electrical power consumption is obtained by accounting for the overall electromechanical efficiency of the compressor drive. The performance of the heat pump is finally quantified through the coefficient of performance, defined as:

$$\text{COP}_{\text{cycle}} = \frac{\dot{Q}_{\text{cond,tot}}}{\dot{W}_{\text{cmp}}}. \quad (5)$$

Compressor performance is modelled through a normalized performance map reconstructed for a centrifugal compressor from reference data available in the literature [7] and showed in Figure 4. The nominal reference point of the map is defined to coincide with the on design operating condition of the thermodynamic cycle. In this formulation, the on design operating point corresponds, by construction, to a unitary map efficiency, while the map describes relative efficiency variations with respect to changes in operating conditions. The effective compressor efficiency is then obtained by scaling the map based relative efficiency with the nominal isentropic efficiency assumed for the reference condition, $\eta_{\text{is,nom}} = 0.8$.

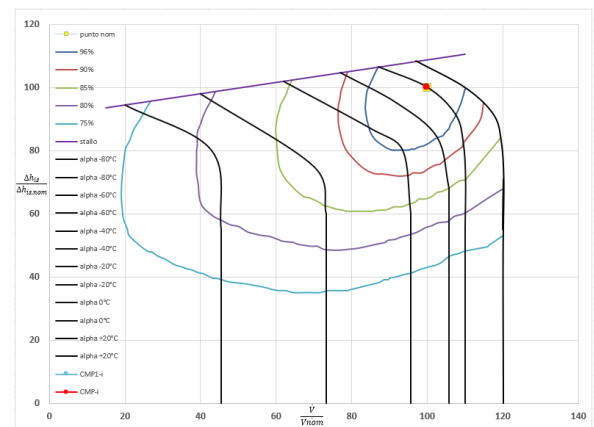


Figure 4: Operating points of the compressors on the performance map.

Heat Exchangers Sizing Methodology

Heat exchangers are described through mass and energy balances coupled with literature correlations for convective heat transfer and phase-change processes. Shell and tube heat exchangers are designed according to the TEMA standard classification, which is adopted to define the constructive layout of the evaporator, condenser and subcooler. The heat transfer processes are modelled by distinguishing single-phase and two phase regions, and by applying established correlations [8]:

- Zukauskas correlation for single phase cross flow convection on the shell side;
- Gnielinski correlation for internal forced convection on the water side;
- Rohsenow correlation for nucleate pool boiling in the evaporator;
- Nusselt theory for film condensation in the condenser.

For single phase sections, the internal and external heat transfer coefficients, $h_{i,int}$ and $h_{i,ext}$, are obtained by discretising the thermodynamic path of the fluids and averaging local values in order to account for property variations along the heat exchangers. The overall heat transfer coefficient U_i is then obtained through a thermal resistance network including internal and external convection, wall conduction and fouling resistances, all referred to the external outer diameter D_o .

For each heat exchanger section i , the required heat transfer area is computed from the imposed thermal duty as:

$$A_{req,i} = \frac{\dot{Q}_{req,i}}{U_i \Delta T_{lm,i} F_i}, \quad (6)$$

where $\Delta T_{lm,i}$ is the logarithmic mean temperature difference and F_i is the correction factor.

The geometric sizing is performed through an iterative search over a bounded design space in terms of number of tubes N_i and total tube length L_i . For each candidate configuration, the available heat transfer area, referred to D_o is evaluated as:

$$A_{eff,i} = N_i \pi D_o L_i \quad (7)$$

and compared with the required one. Feasible solutions are selected by simultaneously satisfying the area constraints of all thermal sections

and the final design is chosen by minimising the total exchanger volume.

The wastewater heat exchanger (EHX_1) is not geometrically designed using standard correlations due to its non standard in sewer configuration. It is instead modelled through an equivalent thermal conductance UA_{EHX_1} identified under on design conditions from the wastewater intermediate loop energy balance.

4.2. Off Design Procedure

Algorithm 2 Off design solution workflow

```

1: Read time-dependent boundary conditions
2: Initialise  $\mathbf{x}^{(0)} = [P_{evap}, P_{cond}, \Delta T_{sub}]^T$ 
3: External solver: CNLE_DEF
4: repeat
5:     Call USERFUNC_DEF( $\mathbf{x}^{(k)}$ )
6:     Call Compute_cycle_Iter
7:      $T_4$  iteration and cmps map integration
8:     Update external temperatures
9:     Recompute  $U_j$ ,  $\Delta T_{lm,j}$  and  $Q_{hex,j}$ 
10:    Enforce physical constraints
11:    Construct residual vector  $\mathbf{F}(\mathbf{x}^{(k)})$ 
12:    Update  $\mathbf{x}^{(k+1)}$  via Newton correction
13: until  $\|\mathbf{F}(\mathbf{x})\| < \varepsilon$ 
14: Verify global energy balances
15: Compute performance indicators

```

Formulation of the Off-Design Problem

The off design modelling framework evaluates the thermodynamic response of the wastewater source heat pump under time varying boundary conditions, as both wastewater availability and district heating demand vary over time. The cycle adapts to these variations through changes in its internal operating variables, while compressor operation is restricted to the validated map region and positive driving temperature differences are enforced in all exchanger sections.

Under off design operation, the following regulation principles are adopted:

- Heat exchanger geometries are fixed at their on design values;
- the wastewater heat exchanger is modelled with constant conductance UA_{EHX_1} from on design;
- the intermediate loop flow rate is fixed, while wastewater flow rate and inlet temperature vary;
- refrigerant mass flow rate is regulated via inlet guide vanes (IGVs);
- residual demand is supplied by the auxiliary electric boiler when heat pump limits are reached;

- heat transfer coefficients U are updated at each operating point.

The off design problem is formulated as a coupled non linear algebraic system enforcing thermodynamic cycle balances and heat exchanger thermal closure with fixed geometry. The operating point is obtained by solving:

$$\mathbf{F}(\mathbf{x}) = \mathbf{0}, \quad (8)$$

where \mathbf{x} is the unknown vector defined as:

$$\mathbf{x} = [P_{\text{evap}} \quad P_{\text{cond}} \quad \Delta T_{\text{sub}}]^T \quad (9)$$

and each residual enforces thermal consistency between the heat exchanger model and the refrigerant enthalpy variation:

$$F_i(\mathbf{x}) = U_i A_i \Delta T_{\text{lm},i} - \dot{m} \Delta h. \quad (10)$$

Off Design Routines Solution

The off design solution is organised as a three-level iterative structure that separates numerical resolution from physical modelling.

Level 1 corresponds to an external non linear solver, `CNLE_DEF`, which solves the non linear system reported in Equation 8 and 10, updating the unknown vector \mathbf{x} and using a Newton type iterative method. The solver operates purely at a numerical level and interacts with the thermodynamic model exclusively through calls to a residual evaluation function.

Level 2 is implemented in `USERFUNC_DEF`, which represents the physical core of the off design model. For a given \mathbf{x} from `CNLE_DEF`, it:

(i) reconstructs the thermodynamic cycle, (ii) computes refrigerant mass flow rates and evaluates compressor operation, (iii) updates external temperature levels and recomputes heat transfer coefficients and overall U values, (iv) evaluates heat exchanger thermal duties $Q_{\text{ehx},i}$, (v) enforces physical constraints on compressors and heat exchangers, (vi) constructs the residual equations F_1 , F_2 and F_3 enforcing thermal closure between refrigerant enthalpy variations and fixed area heat exchanger performance.

Level 3 consists of an internal fixed point iteration, `Compute_cycle_Iter`, used in `USERFUNC_DEF` and embedded within the cycle evaluation, ensuring convergence of the high-pressure compressor outlet temperature and of

compressor efficiencies obtained from interpolated performance maps. This internal closure is completed before residual construction and is fully decoupled from the external solver. Starting from an initial guess $\mathbf{x}^{(0)}$, the three level structure returns the converged operating vector \mathbf{x} , the full set of thermodynamic states, heat duties, compressor powers and COP, while enforcing energy balances and physical constraints.

5. On - Off Design And Sizing Results

5.1. On Design and Sizing Result

The on design simulation computes all thermodynamic state points of the cycle, showed in Table 2 and determine the nominal operating conditions. The main result are showed in Table 3:

Point	T [K]	P [MPa]	h [kJ/kg]	s [kJ/kgK]	x
P1	278.150	0.216	388.75	1.691	–
P2	324.505	0.819	420.76	1.711	–
P3	322.279	0.819	418.41	1.704	–
P4	367.604	2.266	442.22	1.717	–
P5sub	341.150	2.232	296.93	1.310	–
P6	315.650	0.819	296.93	1.319	0.250
P7	315.650	0.819	258.72	1.198	–
P8	315.650	0.819	411.38	1.681	–
P9	273.689	0.221	258.72	1.215	0.315

Table 2: Thermodynamic state points.

Performance	Value
\dot{Q}_{cond} [kW]	2505.269
\dot{Q}_{evap} [kW]	1681.012
\dot{Q}_{ww} [kW]	1676.024
$W_{\text{comp,ele}}$ [kW]	867.639
$W_{\text{pump,ele}}$ [kW]	7.125
COP _{system} [-]	2.864

Mass flow rates	[kg/s]
\dot{m}_{cond}	17.244
\dot{m}_{evap}	12.927
\dot{m}_{int}	99.75
\dot{m}_{water}	29.820

Cycle variables	
T_{cond} [K]	358.150
T_{evap} [K]	278.150
ΔT_{sub} [K]	16.99

Table 3: Main on design results.

Heat exchanger sizing results are reported in the Tables 4, with the corresponding quantitative T - Q diagrams shown in the Figure 5; here Q denotes the steady state heat duty, while \dot{Q} is used elsewhere in the analytical formulation.

Heat Exchanger	A_{ht} [m ²]	N [-]	L [m]	V [m ³]
Evaporator	1022.671	9600	1.78	2.968
Superheater	58.602	9600	0.102	2.968
Desuperheater	112.106	8920	0.21	1.577
Condenser	421.732	8920	0.79	1.577
Subcooler	160.989	2690	1	1.577

Table 4: Heat exchanger sizing results.

A_{ht} is the effective heat transfer area. Evaporator superheater and desuperheater condenser

share the same exchanger (same N , different L), while the subcooler is separate.

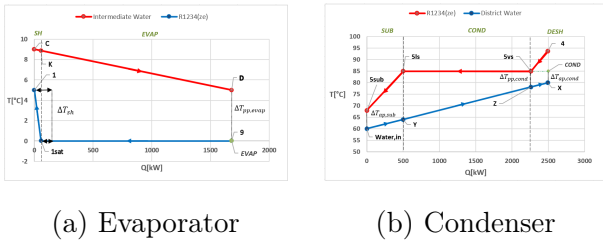


Figure 5: T - Q diagrams of the evaporator and condenser.

5.2. Off Design Result

The off-design solver is applied to three demand levels [$\dot{Q}_{low} = 0.6 \dot{Q}_{nom}$, \dot{Q}_{nom} , $\dot{Q}_{high} = 1.10 \dot{Q}_{nom}$], returning the converged operating variables, heat duties and compressor performance. Variables result are summarised in the Table 5.

The corresponding compressor operating points are reported on the performance maps for each load condition, as showed in Figure 6.

Load	P_{evap} [MPa]	P_{cond} [MPa]	ΔT_{sub} [K]	COP [-]
Low	0.2533	2.0014	16.4409	2.771
Nominal	0.2164	2.2325	16.9932	2.865
High	0.2083	2.2663	16.948	2.729

Table 5: Off design operating variables and performance indicators.

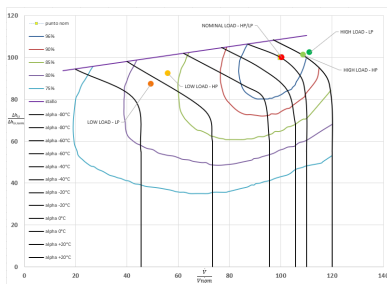


Figure 6: Compressor performance maps with operating off design points.

The off design model reproduces the nominal point, confirming consistency. At partial load, both pressures decrease and compressors operate far from their optimal region, reducing efficiency and COP. At overload, higher compression ratios further penalise compressor efficiency, again lowering the COP.

6. Annual CO₂ Assessment

Building upon the validated on and off design modelling framework, the analysis is extended to annual simulations in order to assess the environmental performance of the complete hybrid system in Figure 1 under realistic conditions and to identify the district heating integration level that maximises annual CO₂ emission savings for the given wastewater availability and heat pump sizing.

The annual assessment considers the simultaneous variability of both the wastewater-side boundary conditions and the district heating thermal demand. On the source side, hourly profiles of wastewater inlet temperature and mass flow rate are reconstructed from available literature datasets [9] and processed to obtain coherent annual time series representative of the considered urban context. On the demand side, an hourly thermal load profile provided for a residential district heating network is adopted as reference condition and identified with a demand scaling factor $\alpha = 1$. To maintain computational efficiency, both yearly datasets are organised into 3°C ambient temperature ranges, constructing hourly profiles for each class.

In order to investigate different integration levels between the heat pump and the district heating network, the reference demand profile is scaled within the range $0.8 \leq \alpha \leq 4.0$. For each value of α , annual simulations are performed at hourly resolution using the off design model. The system operates in hybrid mode, with the wastewater heat pump covering the load within its limits and an electric boiler supplying residual demand.

For each annual simulation performed at a given α , which correspond to a required annual thermal energy, the total CO₂ emissions of the hybrid system are calculated by aggregating the hourly contributions of both the heat pump and the electric boiler. These emissions are then compared with a reference scenario in which the same annual thermal demand is entirely supplied by a natural gas boiler, allowing the evaluation of the net annual CO₂ emission savings.

Both CO₂ emissions calculations accounting the specific emission factors:

$$\begin{cases} e_{el} = 215.9 \text{ kgCO}_2/\text{MWh}_{el} \\ e_{GN} = 213.06 \text{ kgCO}_2/\text{MWh}_{fuel} \end{cases} \quad (11)$$

consistent with national reference data [10]. The equivalent emission factors for the electrically driven technologies are defined in unified form as:

$$e_{i,h} = \frac{e_{el}}{\text{COP}_{i,h}}, \quad i \in \{\text{HP, boiler}\}, \quad (12)$$

where $\text{COP}_{\text{HP},h}$ is the hourly coefficient of performance obtained from the off-design simulations, while $\text{COP}_{\text{boiler}} = 1$ is assumed for the electric boiler.

The equivalent emission factor of the reference natural gas boiler is instead given by:

$$e_{\text{GN,ref}} = \frac{e_{\text{GN}}}{\eta_{\text{boiler,ref}}}, \quad (13)$$

where $\eta_{\text{boiler,ref}} = 0.95$ [11].

At this stage, the annual CO_2 emissions of the hybrid configuration are directly compared with those of the reference natural gas scenario, and their difference provides the annual CO_2 emission savings for each demand scaling factor α . With this procedure, for each considered α , the total annual heat demand and supply ($\text{MWh}_{\text{th}}/\text{year}$) and the corresponding CO_2 savings ($\text{tonCO}_2/\text{year}$) are determined.

7. Final Results and Conclusions

The results shown in Figure 7 highlight the relationship between district heating demand and achievable CO_2 emission savings. While the annual thermal energy supplied increases proportionally with the scaling factor α , ranging from approximately 10.6 to 53.2 $\text{GWh}_{\text{th}}/\text{year}$, the corresponding CO_2 reduction exhibits a clear maximum within the investigated interval.

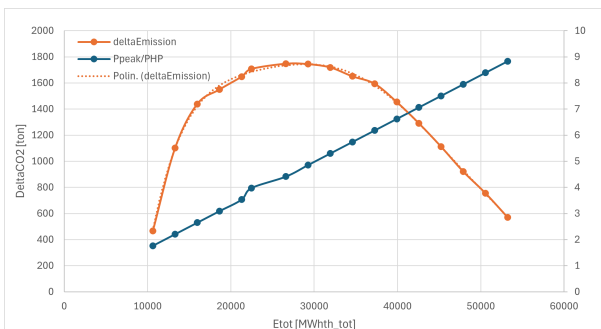


Figure 7: Annual thermal energy and CO_2 savings as a function of α .

The maximum annual emission saving of 1747.5 tCO_2/year is obtained for $\alpha = 2$, corresponding to an annual heat supply of approximately 26.612 $\text{GWh}_{\text{th}}/\text{year}$. Beyond this point, the increasing contribution of the auxiliary electric boiler under peak-load operation reduces the marginal environmental benefit, as reflected by the monotonic growth of the $P_{\text{peak}}/P_{\text{HP}}$ ratio. These findings demonstrate the existence of an optimal district heating demand level for which the integration of the wastewater heat pump maximises annual CO_2 emission savings under fixed wastewater availability and installed capacity.

Overall, this thesis develops a robust thermodynamic framework for on design sizing and off design operation of wastewater source heat pumps and proposes a systematic procedure to identify their optimal integration within an urban district heating network in order to maximise environmental benefits. The methodology thus provides a practical tool to support sizing and planning decisions in urban heat decarbonisation strategies.

References

- [1] Intergovernmental Panel on Climate Change (IPCC), “Climate change 2022: Mitigation of climate change. contribution of working group iii to the sixth assessment report,” 2022.
- [2] ENEA, “Recupero di energia termica da reflui urbani per applicazioni di teleriscaldamento,” Agenzia Nazionale per le Nuove Tecnologie, l’Energia e lo Sviluppo Economico Sostenibile, Tech. Rep., 2019.
- [3] MM S.p.A., “Progetto sperimentale per un impianto pilota di cogenerazione asservito alla centrale ap salemi – relazione generale,” Metropolitana Milanese S.p.A., Tech. Rep., 2017.
- [4] —, “Studio di fattibilità per il recupero di energia termica da reflui fognari mediante pompe di calore in edifici erp,” Metropolitana Milanese S.p.A., Tech. Rep., 2019.
- [5] K. E. Herold, R. Radermacher, and S. A. Klein, *Absorption Chillers and Heat Pumps*, 2016.

- [6] R. Ben Jemaa, R. Mansouri, and A. Bellagi, “Energy and exergy analysis of r1234ze as a low-gwp refrigerant,” *International Journal of Hydrogen Energy*, 2017.
- [7] Atlas Copco, “Centrifugal compressor performance maps and technical documentation,” Atlas Copco AB, Tech. Rep., 2020.
- [8] T. L. Bergman, A. S. Lavine, F. P. Incropera, and D. P. DeWitt, *Fundamentals of Heat and Mass Transfer*, 2011.
- [9] Stadtentwässerungsbetriebe Köln, “Wwtp köln-weiden wastewater flow rate dataset,” 2020.
- [10] ISPRA, “Fattori di emissione di CO_2 del settore elettrico nazionale,” 2025.
- [11] European Commission, “Commission regulation no 813/2013 of 2 august 2013 implementing directive 2009/125/ec with regard to ecodesign requirements for space heaters and combination heaters,” 2013.